Environmental Health Perspectives
Vol. 85, pp. 331-352, 1990

Pathology Working Group Review of Selected Upper Respiratory Tract Lesions in Rats and Mice

by R. R. Maronpot*

The collected comments and pathologic diagnoses of several pathologists are summarized for 18 cases in which lesions were induced in the upper respiratory tract of rats and mice. Specific neoplastic and nonneoplastic lesions of the nose and trachea are described and discussed, and opinions regarding pathogenesis and biologic significance of the lesions are presented. The anatomic and pathophysiologic complexities of the rodent nose in relation to lesion development following inhalation or systemic exposure to xenobiotics are important considerations in the genesis of pathologic changes in this organ.

Introduction

A Pathology Working Group (PWG) review of selected upper respiratory tract lesions was held on the afternoon of September 14, 1988. Symposium speakers and invited guests had the opportunity to discuss the histologic lesions present in 18 cases selected from rat and mouse toxicity and carcinogenicity studies. Since several important concepts were discussed during this PWG session, a decision was made to publish some of the comments and document the selected lesions for the benefit of investigators and pathologists specializing in the upper respiratory tract. Over 20 pathologists participated in this PWG session. Comments are reported without attribution. Most of the information presented below was confirmed by examining notes provided by several PWG participants.

Cases 1 and 2

History

Case 1 represents a longitudinal section of trachea and Case 2, a section from the tracheal bifurcation from $B6C3F_1$ mice that had inhaled 40 ppm formaldehyde for several weeks. These two mice became moribund and were sacrificed prior to termination of the National Toxicology Program (NTP) 13-week inhalation study of formaldehyde vapor.

Histological Findings and Comments

Case 1 represents a midsagittal section of trachea. Thick bands or bridges of mature collagen lined by proliferative and metaplastic epithelium traversed the tracheal lumen (Plates 1-3). Epithelium lining these connective tissue bridges and the tracheal wall was metaplastic, hyperplastic, and sometimes dysplastic (Plate 4).

In Case 2 similar changes were present at the tracheal bifurcation, but the connective tissue proliferation was less mature and extensive. Although some areas in these cases are suggestive of papillomas, there was no clear evidence for either benign or malignant neoplasia.

The lesions present in Cases 1 and 2 were considered a toxic response to repeated acute insult. The postulated pathogenesis of these lesions was believed to start with destruction of epithelial surfaces followed by subsequent fibrosis and reepithelialization. Some reversibility or remodeling of intraluminal lesions was believed to occur, with a slow and incomplete resolution of the smaller, milder lesions. These intraluminal lesions had some similarity to those seen after exposure to 3-methyl indole and methyl isocyanate. The epithelial changes may be considered as proliferative with moderate to marked dysplastic changes bordering on preneoplasia. Stripping of the epithelial surface, particularly if there was damage to the basement membrane, was associated with increased connective tissue proliferation in the lamina propria and secondary increased epithelial proliferation. As the epithelium is stimulated to proliferate, at times it may grow into the lamina propria. If the denuding of the epithelial surface is not complete and progenitor cells are available for epithelialization of the damaged mucosa, the proliferative response may progress to hyperplasia and dysplasia without connective tissue proliferation. Study of the acute response to agents that cause this sort of damage may provide information about the significance of acute histologic changes with respect to which changes are warning signals indicating that, if exposure continues, malignancy may result.

*National Toxicology Program, National Institute of Environmental Health Sciences, P.O. Box 12233, Research Triangle Park, NC 27709.

It is tempting to postulate a pathogenesis of lesion development on the basis of examining mild to moderate to severe lesions, such as in these two cases. However, without a longitudinal temporal sampling of the entire process, we must appreciate that any conclusions regarding pathogenesis derived from a relatively static sample are speculative, requiring further experimental confirmation.

Diagnoses

Intraluminal fibrosis (synonym: fibroepithelial bridges, chronic fibroepithelial change, tracheitis obliterans), hyperplasia, metaplasia, and dysplasia.

Case 3

History

The section is from the nose of a Fischer 344 rat that had inhaled formaldehyde in the Chemical Industry Institute of Toxicology's (CIIT) 2-year carcinogenicity study.

Histological Findings and Comments

Epithelial metaplasia, particularly along the lateral wall and septum (Plate 5), was typical for formaldehyde exposure. Depending on the extent of exposure, the lesions along the epithelial surfaces may be patchy. Above the dorsal meatus, there was olfactory epithelial degeneration with attendant regeneration, squamous metaplasia of the mucosal epithelium, and infolding of the basal epithelial layer with glandlike formations (Plate 6). The widespread intravascular thrombosis is not typically associated with formaldehyde exposure but was prominent in this case (Plate 7). Secondary bony changes include thickening and proliferation of woven bone replacing the normal compact bone of the turbinates (Plate 7).

Importance of lesion distribution as a function of exposure to a specific chemical was underscored by this example. Lesion distribution in this case was classical for gas irritants. Olfactory and bone lesions are similar to those reported for dimethylamine. There are two types of squamous metaplasia that can been seen after insults such as this: compact and large epitheloid cell. Keeping track of these differences as one examines successive studies may provide a basis for eventually assessing the differential significance of the two types of metaplasia.

In light of the distribution of normal epithelial types, a necessary prerequisite for establishing the presence and type of metaplastic changes in a given region was to consistently sample sections from the noses of controls. At this level of the nose, the lateral walls and the maxillary turbinates normally lined by an epithelium that is not typically ciliated respiratory epithelium but, rather, is transitional or nonciliated pseudostratified cuboidal epithelium. The extension of olfactory epithelium into the anterior region of the dorsal meatus is apparently age and, possibly, strain dependent. In addition to differences between very young and more mature animals, there are also differences in the anterior extension of olfactory epithelium between rats and mice.

Literally dozens of diagnostic terms can be applied to the complex constellation of changes present in the nose in situations represented by a case such as this one. The pathologist can create confusion and extra work if too many diagnoses are used to characterize the changes present. The tissues that get diagnosed and graded become a judgment, but for practical considerations, should be limited to basic or major changes, with secondary and minor changes being described in a summary narrative of the pathologic effects.

While evaluating treatment effects in histologic slides such as this, a strong case against blind reading can be made. Blind documentation of the wide array of lesions present in a case such as this could prevent the pathologist from focusing on relevant changes because he or she would feel compelled to document everything.

Diagnoses

Hemorrhagic rhinitis, olfactory degeneration, osteofibrosis, intravascular thrombosis, erosions, ulcers, squamous metaplasia, fusion of nasal turbinates.

Case 4

History

The section was from the nose of a Fischer 344 rat in the CIIT 2-year formaldehyde carcinogenicity study.

Histological Findings and Comments

A large and highly keratinized papillary proliferation of squamous epithelium extended into the nasal cavity from the dorsolateral wall (Plate 8). Although the pattern of the proliferative growth with its branching connective tissue core was consistent with squamous cell papilloma, there was sufficient histologic evidence of local invasion to consider this lesion to be malignant. In addition, there was evidence of mild dysplasia, and a large number of mitoses were present in the proliferating epithelium. Prominent keratinization in nasal epithelial proliferations is typically seen in situations where the treatment is associated with development of carcinoma.

Other changes noted included epithelial attenuation and squamous metaplasia with accompanying rhinitis affecting the nasal septum (Plate 9), as well as the naso- and maxilloturbinates. Thickening of turbinates by proliferating woven bone accompanied the inflammatory and metaplastic changes.

Diagnoses

The consensus of the working group was for a malignant lesion, squamous cell carcinoma of the lateral wall, although most agreed it was a borderline malignancy. The

changes in turbinate bone were diagnosed as osteofibrosis. Other diagnoses included rhinitis and metaplasia.

Case 5

History

The section of nose was from a Fischer 344 rat in the CIIT 2-year formaldehyde inhalation study.

Histological Findings and Comments

Squamous epithelial proliferation and formation of keratin pearls was evident throughout this section of the nose (Plate 10). In general, the proliferating epithelial cells were well differentiated with only a few areas showing nuclear pleomorphism. Many keratin pearls associated with the proliferating squamous epithelium were evident throughout the mucosa of the nasal septum, maxillo-, and nasoturbinates (Plate 11), dorsal arches, and lateral wall, as well as in the vomeronasal organ. Invasion of a markedly thickened frontal bone by proliferating and keratinizing tumor cells was obvious in the section (Plate 12).

There was some discussion among the working group about how one determines when such a case represents a primary or metastatic event. In the context of the formaldehyde study, the proliferating squamous cells may be regarded as arising in the nasal cavity. However, in other situations it is possible for squamous cell carcinomas of the skin, oral cavity, or Zymbal gland to invade or metastasize to the nose. Depending upon the extent of involvement, establishing a site of origin could theoretically be difficult. Even in the present case, the widespread involvement of the nose, including the vomeronasal organ, suggests localized metastases. Many of the lesions present may represent lymphatics and blood vessels filled by metastatic squamous cell carcinoma.

Diagnoses

Squamous cell carcinoma, rhinitis.

Case 6

History

The section of nose was from a Fischer 344 rat in the CIIT 2-year dimethylamine inhalation study.

Histological Findings and Comments

There was olfactory epithelial degeneration affecting the mucosa of the dorsal arches (Plate 13). Remaining sustentacular cells were conspicuous because of the loss of the sensory cell layer. Pseudogland formation was present in the remaining surface epithelium (Plate 14); this was commonly observed in degenerating olfactory epithelium. Dilated Bowman's glands were present in the underlying lamina propria (Plate 14). As a manifestation of mild hyperplasia, invaginations of respiratory epithelium were present along dorsal aspects of the nasal septum (Plate 13).

At this level of the nasal cavity, affected areas reflected degenerative changes associated with regions of major airflow. The degenerated olfactory epithelium in the dorsal arches does not regenerate in the face of continued exposure. This type of response is typically seen with cytotoxic agents. A common histologic artifact frequently produced in nasal sections is characterized by overlapping of the frontal bone and the olfactory mucosa (Plate 13). This ubiquitous artifact may preclude adequate assessment of olfactory mucosal lesions. Hyperostosis was also present in this case (Plate 15).

Eosinophilic cytoplasmic inclusions that represented proteinaceous deposits in dilated rough endoplasmic reticulum were present in the columnar epithelial cells covering the septum (Plate 16). These cytoplasmic inclusions have been seen in control and treated animals in many studies and are neither PAS or alcian blue positive. The frequency of this change increases dramatically in aging animals, and the frequency and severity may be exacerbated by treatment. Both the eosinophilic cytoplasmic inclusions and similar crystalline material that is sometime observed are more often a response to chronic (90 days or longer) insult, rather than an acute response. However, similar cytoplasmic changes have been seen in monkeys following ozone exposure for just 9 days. Eosinophilic cytoplasmic inclusions are generally not associated with inflammation, but are typically associated with secretory cells. These changes frequently localize in three areas: sustentacular cells of the olfactory epithelium, glands at the olfactory-respiratory junction lining the dorsal meatus, and in the respiratory epithelium, particularly along the septum. It has been suggested that these eosinophilic inclusions may be a hormonal response of some sort, or may be associated with ammonia in the microenvironment. The issue as to whether or not to document this change as a lesion is a judgment call generally influenced primarily by severity of the change.

Diagnoses

Olfactory epithelial degeneration. Cytoplasmic inclusions.

Case 7

History

Three cross-sections were from the nose from a Fischer 344 rat in the CIIT dimethylamine inhalation study.

Histologic Findings and Comments

Of the three cross-sectional levels of the nose (Plates 17–19) on the slide, the middle section was without an

intact nasal septum, corresponding to the gross observation of nasal septal perforation. At the level of the perforated septum there was atrophy of the remnants of the nasal septum as well as the nasal and maxillary turbinates. These changes were accompanied by inflammation and squamous metaplasia of the respiratory epithelium. In the olfactory mucosa overlying the dorsal meatus in the most posterior section, there was mild cystic dilation of Bowman's glands, some of which contained inspissated material, as well as hyperplasia of the glands (Plate 20). Other changes included degeneration of olfactory epithelium with only basal and sustentacular cells remaining and focal invagination of the olfactory epithelium (Plate 21).

This spectrum of changes was nonspecific, which was expected as a consequence of exposure to an irritating vapor. The loss of olfactory sensory neurons was marked. It is typical for olfactory sensory neurons to be among the first cells to degenerate following exposure to a cytotoxic vapor. The identification of the remaining olfactory epithelial cells can sometimes be problematic. Use of cytochemical stains and electron microscopy may be of help in defining the relatively resistant cell population. Discontinuation of exposure can be expected to be followed by a repopulation of the olfactory epithelium with all normal cell components ultimately being regenerated. The origin of the regenerated sensory cells remains unknown with no definitive proof of their origin from either basal, sustentacular, or Bowman's gland cells.

Necrosis of olfactory epithelium with a sparing of Bowman's glands, which occurred in this case, typically leads to regeneration of olfactory epithelium after cessation of exposure. This sort of regeneration has been seen with acetaldehyde exposure. In situations where there is loss of Bowman's glands, there may be no regeneration of olfactory sensory epithelium. This has caused some to speculate that Bowman's glands or the neck of Bowman's glands contain the progenitor cell population for regeneration of the olfactory epithelium.

Diagnoses

Septal perforation, turbinate atrophy, squamous metaplasia, diffuse chronic rhinitis, olfactory degeneration.

Case 8

History

The section of nose was from a B6C3F$_1$ mouse in the NTP 2-year inhalation study of 1,2-dibromo-3-chloropropane.

Histological Findings and Comments

Two proliferative lesions were present on the nasoturbinates; one was prominent (Plate 22) and the other smaller. There appeared to be a mixture of epithelial proliferation in the prominent lesion. Proliferating larger squamoid cells had nuclei perpendicular rather than parallel to the basement membrane (Plates 23 and 24). These squamoid cells were similar to those observed to proliferate in hamsters following their exposure to diethylnitrosamine in hamsters. Smaller more basal appearing cells also proliferated (Plates 23 and 24). There was nuclear pleomorphism and hyperchromaticity in glandular cells (reactive mucosal glands) located deeper in the thickened mucosa (Plate 25). Similar nuclear pleomorphism is commonly observed in the mucosal glands as a general response to insult.

While there was considerable proliferation into the nasal cavity lumen, elements of the proliferative response appeared to have resulted from downgrowth of basal cells of the surface epithelium which is illustrated in the smaller of the two primary lesions (Plate 24). Because of the anatomic location of these focal proliferative lesions and the morphologic appearance of the proliferating cells, an origin from the transitional or nonciliated respiratory epithelium was proposed. Squamous cells would be expected to orient themselves parallel to the basement membrane. The consensus was that these focal proliferations represented benign lesions.

Similar proliferative lesions occur in humans and may have papillary and squamoid features. If glandular structures are present, but the squamous component predominates, they are diagnosed as a squamous cell neoplasms. If the glandular features are sufficiently dominant, they are considered adenosquamous neoplasms.

Changes in the nasal septal mucosa were considered to represent a downgrowth of surface epithelium into the lamina propria. Nuclear pleomorphism and hyperchromaticity were present in the nasal septal mucosal glands.

Diagnoses

Adenomas (synonym: polypoid adenomas, epidermoid adenomas). Hyperplasia of subepithelial glands. There was a long discussion regarding the term "epidermoid adenoma" versus "polypoid" or "papillary adenoma" but no clearly preferred diagnostic term was agreed upon.

Case 9

History

The section of nose was from a B6C3F$_1$ mouse in the NTP 2-year propylene oxide inhalation study.

Histological Findings and Comments

Close inspection at low magnification revealed a predominantly unilateral thickened maxillary sinus mucosa (Plate 26). The thickening resulted from a mild inflammation and a pronounced proliferative response comprised of epithelial cells forming glands. The proliferating glands were lined by well-differentiated ciliated cells. Because of the well-differentiated nature of the proliferating cells, this lesion is compatible with a hyperplasia.

However, there was clear evidence of an invasion of adjacent skeletal muscle (Plate 27) and perineural tissue (Plate 28) by the well-differentiated ciliated glands. While the skeletal invasion might be regarded as analagous to endometriosis, adenomyosis, or proliferative ileitis in hamsters, the presence of proliferating glands around nerve bundles is not compatible with a typical benign proliferative response. Thus, the proliferation was reluctantly considered a malignant maxillary sinus gland tumor.

Everyone agreed that this was a one-of-a-kind lesion that probably had nothing to do with treatment. The possibility that such a response might be secondary to viral or mycoplasmal infection was raised.

It was noted that this lesion was similar to some rare tumors in humans that appear as cystlike structures that are comprised of respiratory epithelium, are histologically benign, but show invasiveness, and reoccur following treatment. In other words, their biological behavior is like that of a malignant neoplasm.

Diagnoses

While the consensus was for a maxillary sinus gland tumor, probably an adenocarcinoma, everyone was concerned about the benign and well-differentiated nature of the epithelium with cilia. At least four participants did not consider this growth to represent a neoplasm and preferred the diagnosis of harmatoma.

Case 10

History

The section of nose was from a Fischer 344 rat in the NTP 2-year inhalation study of 1,2-dibromoethane.

Histological Findings and Comments

Two of the three proliferative lesions present in this case were large polypoid proliferations arising from the lateral wall on either side of the nasal cavity (Plate 29). One was considered a papillary adenoma (alternate terminology was an epidermoid papilloma) and was comprised of multilayered cuboidal to columnar cells. The group commented that papillary adenomas can become quite large. The second lesion was similar, but in addition to proliferating cuboidal cells, also had areas of squamous cell metaplasia and other regions comprised of proliferating squamoid cells, believed to be derived from the nonciliated (transitional) respiratory epithelium of the lateral wall. This neoplasm was considered malignant, based on microscopic areas of early invasion in some of the serial sections.

The subepithelial mucosa of the nasal septum was characterized by a locally invasive proliferation of basophilic epitheliallike cells throughout the mucosa in addition to perineural invasion (Plate 30). The proliferating cells (Plate 31) did not form any recognizable structures and were generally felt to be neuroepithelial cells from the olfactory area of the nose. Neuroepithelial neoplasms tend to grow anteriomedially in the nasal septum. A similar type of proliferation, but with brain metastases, has been observed following exposure to high doses of vinyl chloride.

Diagnoses

Olfactory neuroepithelioma in the nasal septum. Adenocarcinoma and polypoid adenoma in anterior nasal cavity.

Case 11

History

The section of nose was from a Fischer 344 rat in the NTP 2-year dimethylvinyl chloride study. The route of exposure was by gavage.

Histological Findings and Comments

A large mass, which on low magnification had a blue stippled granular texture and an amorphous pattern, had completely filled one-half of the nasal cavity at this level of sectioning (Plate 32). Areas of necrosis were evident within this large proliferative mass. At higher magnification delicate connective tissue septa irregularly compartmentalized proliferating anaplastic epithelial cells. In some areas of the neoplasm, tumor cells were aligned perpendicularly along the thin connective tissue septa to where they were attached by a cytoplasmic filament (Plate 33). Thus, these cells resembled olfactory sustentacular epithelium. Based upon growth pattern and cytomorphologic features, this neoplasm was considered of olfactory neuroepithelial origin.

The participants generally agreed to classify all olfactory neoplasms as neuroepitheliomas and subclassify them as sustentacular, basal cell, sensory cell, or mixed. Such neoplasms are assumed to be malignant unless specified as being benign. True glands and rosettes are rare for olfactory neuroepitheliomas in man, as in the present case.

Because of the prominence of the above neoplasm, it was relatively easy to overlook a papillary proliferation in the nasolacrimal duct (Plate 34). Although this nasolacrimal duct lesion was morphologically consistent with a squamous cell papilloma, some participants felt that there were microscopic areas of localized invasion, and, thus, considered the nasolacrimal duct neoplasm to have early evidence of malignancy.

Diagnoses

The large mass was diagnosed as an olfactory neuroepithelioma of sustentacular cell origin. The consensus diagnosis for the nasolacrimal duct papillary neoplasm was squamous cell carcinoma.

Case 12

History

The section of nose was from a Fischer 344 rat in the NTP 2-year gavage study of dimethylvinyl chloride.

Histological Findings and Comments

There was a large proliferative growth occupying one-half the nasal cavity (Plate 35). The incisor tooth was completely surrounded by the proliferative mass and underwent degenerative changes. The mass was comprised of anaplastic epithelial cells growing in sheets and sometimes had a fusiform appearance (Plate 36). The adjacent nasolacrimal duct was lined by a thickened and irregular layer of stratified squamous epithelium.

There was controversy as to whether this proliferative mass represented one or two neoplasms. Some participants considered that the primary neoplasm was an anaplastic carcinoma and that the changes in the adjacent nasolacrimal duct were secondary. Some felt that the neoplasm arose as a nasolacrimal duct squamous cell carcinoma and argued that there was evidence of transition from stratified squamous cells to anaplastic epithelial cells. Others felt that there was both an anaplastic carcinoma and a nasolacrimal duct neoplasm. All agreed that when presented with such a massive neoplasm, it is difficult to determine the site of origin. Accompanying the neoplastic proliferation was a reactive inflammation and secondary proliferative bony changes.

Diagnoses

Squamous cell carcinoma of nasolacrimal duct with anaplasia or anaplastic carcinoma. (Alternative diagnoses: spindle cell carcinoma, nonkeratinizing carcinoma.)

Case 13

History

The section of nose was from a Fischer 344 rat in an NIEHS experimental study with NNK. NNK [4-(*N*-methyl-N-nitrosamino)-1-(3-pyridyl)-1-butanone] is a tobacco-specific nitrosamine that was administered three times a week for 8 weeks by SC injection. This case was obtained several weeks after cessation of treatment.

Histological Findings and Comments

There was prominent multifocal thickening of the ethmoid turbinates (Plate 37). The thickening consisted of epithelial proliferations in the olfactory mucosa. For the most part, the proliferative changes looked epidermoid or squamoid (Plate 38). In some of these areas of proliferative mucosa there was keratinization of the surface epithelium and prominent desmosomes were visible, suggesting that the proliferating cells were squamous. In other areas of epithelial cell proliferation there was gland formation (Plate 39). It was not clear what the cell of origin was for these proliferative lesions. Some believed the proliferation to be of olfactory basal cell, origin while others favored origin from Bowman's gland cells. This latter opinion was weakened by the paucity of Bowman's glands in the olfactory mucosa. NNK is known to preferentially localize in Bowman's glands and cause necrosis in these structures. The proliferative lesions were sufficiently unusual that an understanding of the disease process was not clarified by the discussion. Opinions ranged from hyperplasia of unspecified olfactory epithelium to carcinoma of Bowman's glands.

To complicate matters, on the contralateral side of the nose, there was evidence of early epithelial hyperplasia, suggestive of an origin from olfactory basal cells (Plate 40), but there was also evidence of hyperplasia of Bowman's glands or the cells in the necks of Bowman's glands (Plate 41). This latter point was deduced from the pattern of proliferation which was seen at regular intervals just beneath the olfactory epithelial basement membrane.

The dorsal arches in the ethmoid area of the nose were characterized by absence of Bowman's glands, degeneration of olfactory epithelium, and respiratory metaplasia of the olfactory mucosa (Plates 42–44).

A proliferative response in the subepithelial mucosa of the nasal septum, similar to that present in Case 10, was considered an olfactory neuroepithelioma by some and was diagnosed hyperplasia of the septal olfactory organ by others.

Diagnoses

The diagnoses for the olfactory turbinate proliferations included olfactory epithelial hyperplasia, olfactory basal cell hyperplasia, epidermoid papilloma (inverted papilloma), and carcinoma *in situ* of Bowman's glands or basal cells. The consensus was that the septal lesion was malignant.

Case 14

History

The section of nose was from a Fischer 344 in an NIEHS experimental study with NNK.

Histological Findings and Comments

The lesion in this section was characterized by a subepithelial thickening of the mucosa above the dorsal meatus. The subepithelial mucosa was infiltrated by poorly formed packets or nests of epithelial-like cells, with evidence of cellular atypia and of perineural invasion (Plate 45). While at least four participants felt that this proliferative response represented hyperplasia, perhaps of Bowman's glands, others felt that this was a carcinoma. Those arguing for hyperplasia felt that the

normal architecture was sufficiently retained to rule out a malignancy. There was no consensus among those calling this a carcinoma as to whether the site of origin was Bowman's glands. The proliferating cells did not closely resemble Bowman's glands. As in the previous case, NNK treatment had caused necrosis of Bowman's glands in this area of the nose.

Diagnoses

These was no clear consensus. Diagnoses were split between hyperplasia and carcinoma. The origin of the proliferative cells was unknown.

Case 15

History

The section of nose was from a Fischer 344 rat in an NIEHS experimental study with NNK.

Histological Findings and Comments

There was a prominent unilateral mass that involved the lateral wall, replaced the olfactory turbinates, and penetrated through the dorsal part of the septum. The mass was largely composed of irregular packets of epithelial cells separated by incomplete, thin connective tissue septa (Plate 46). The histologic appearance of the cells forming irregular packets was similar to that described in Case 11. In some areas the proliferating cells were growing in sheets and had a somewhat fusiform appearance (Plate 47). On the contralateral side of the nose, there were generalized mucosal proliferations similar to those described in Case 12 in addition to inflammatory changes.

Diagnosis

Olfactory neuroepithelioma, sustentacular cell type.

Case 16

History

The section of olfactory portion of the nose was from a Sprague-Dawley rat in the NTP 2-year study of 2,6-xylidine. The chemical was administered in the diet.

Histological Findings and Comments

There was thickening of several ethmoid turbinates and the nasal septum by anaplastic epithelial cells proliferating in the mucosa (Plate 48). The proliferating cells were anaplastic, did not form any recognizable structures, and were locally invasive and destructive (Plates 49 and 50). In some parts of the neoplasm, the neoplastic cells had a fusiform, mesenchymal appearance. Secondary proliferative bony changes were present in some affected turbinates.

Diagnoses

Anaplastic carcinoma. (Alternative diagnosis: carcinosarcoma.)

Case 17

History

The section of olfactory portion of the nose was from a Sprague-Dawley rat in the NTP 2-year study of 2,6-xylidine. The chemical was administered in the diet.

Histological Findings and Comments

A large, unilateral mass containing patches of necrosis and accompanied by rhinitis had effaced the ethmoid turbinates (Plate 51). Portions of the mass were comprised of moderately well-differentiated cuboidal epithelial cells forming glands, consistent with a low-grade adenocarcinoma. Other portions of the mass, at least in the original histologic sections, consisted of relatively solid proliferations of mesenchymal cells consistent with a well-differentiated rhabdomyosarcoma. Between these two relatively pure neoplastic populations, there was an intermingling of the two neoplastic cell types, and well-formed proliferating glands could be seen within areas that were largely rhabdomycosarcoma and vice versa (Plate 52). Special staining and electron microscopy on these tumors during the original evaluation of the 2,6-xylidine study confirmed the striated muscle characteristics of the rhabdomyosarcomas.

Diagnoses

Mixed malignant neoplasm (adenocarcinoma and rhabdomyosarcoma)

Case 18

History

The section of nose was from a Sprague-Dawley rat in the NTP 2-year study of 2,6-xylidine. The chemical was administered in the diet.

Histological Findings and Comments

This mesenchymal neoplasm, which occupied one-half of the olfactory region of the nose, had histologic features consistent with a rhabdomyosarcoma (Plate 53). Unlike Case 17, there were no glandular epithelial elements present in this nasal neoplasm.

Cases 16, 17 and 18 represent the range of nasal neoplasms observed in the 2,6-xylidine study. While development of epithelial neoplasms is known to occur in the

nose of rodents, particularly after chemical exposure, the occurrence of rhabdomyosarcoma is unexpected. None of the participants were aware of any skeletal muscle tissue normally present in the nasal cavity of rodents. However, rhabdomyosarcomas have been reported in the nose of humans. The site of origin of these mesenchymal neoplasms is unknown. Similar neoplasms were not observed in other tissues of affected rats.

Diagnoses

Rhabdomyosarcoma.

PLATE 1. Photomicrograph of a sagittally sectioned trachea from Case 1. The lumen is traversed by epithelial bands of connective tissue (fibroepithelial bridges). H&E.

PLATE 2. Photomicrograph of a midsagittal section of trachea. Fibroepithelial bridges traverse the tracheal lumen. This photomicrograph is a deeper section of the trachea in Plate 1 and is included to demonstrate the ubiquity of the fibroepithelial bridges in an affected mouse. H&E.

PLATE 3. Higher magnification of the intraluminal fibrosis in Plate 2. H&E.

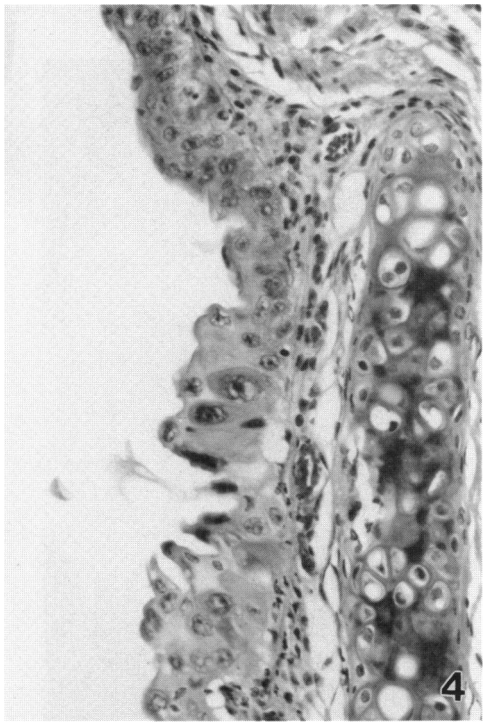

PLATE 4. High magnification near the tracheal bifurcation in Case 2. Dysplastic changes are present in the metaplastic epithelium lining the airway. H&E.

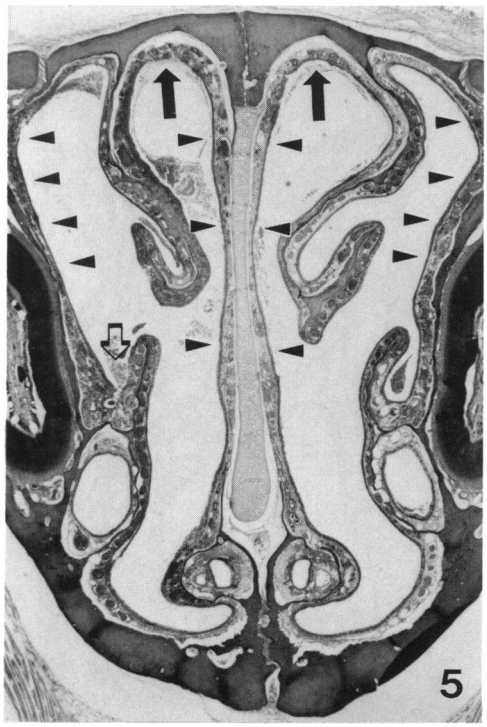

PLATE 5. Photomicrograph of the anterior part of the nose from Case 3. Small arrows indicate the areas of epithelial metaplasia along the lateral walls and the nasal septum. Large arrows indicate the olfactory area at this level of sectioning. Open arrow indicates an adhesion between the maxillary turbinate and the lateral wall. H&E.

PLATE 6. Olfactory area of Plate 5. There is squamous metaplasia of the mucosal epithelium and infolding of the epithelium with formation of glandlike structures. H&E.

PLATE 7. Nasal turbinate from Plate 5. Intravascular thrombosis is indicated by large arrows. Formation of woven bone (small arrows) is present along with normal trabecular bone (open arrow). There is extensive inflammation and epithelial metaplasia. H&E.

PLATE 8. Highly keratinized papillary proliferation arising from the lateral wall of the nose in Case 4. H&E.

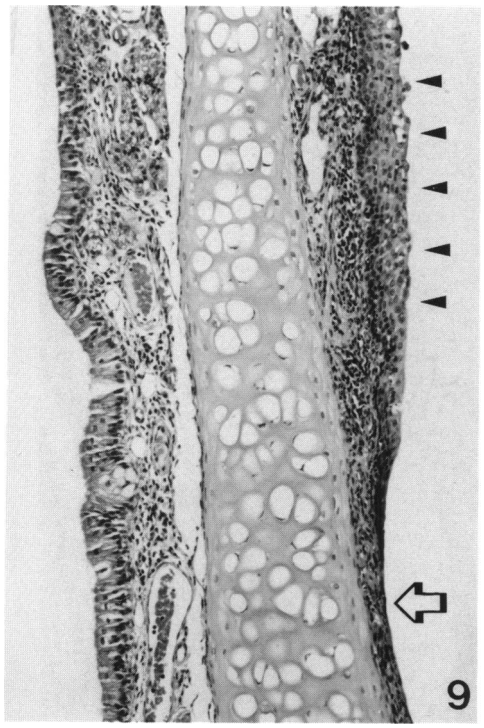

PLATE 9. Nasal septum from Case 4. There is metaplasia of the mucosal epithelium (small arrows) and marked focal attenuation of the epithelial mucosa (open arrow) in addition to a mild to moderate infiltration by inflammatory cells in the lamina propria. H&E.

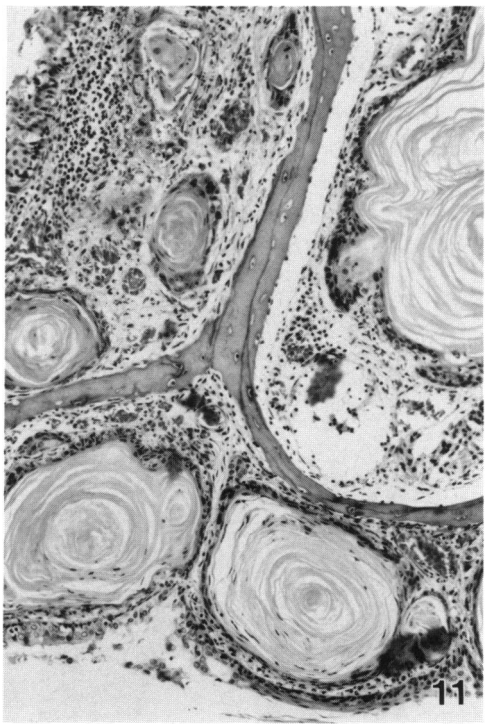

PLATE 11. High magnification of Plate 10 showing keratin pearls in the turbinate mucosa. H&E.

PLATE 10. Photomicrograph of the nose of Case 5. Small arrows indicate formation of keratin pearls by the neoplastic squamous epithelial cells. H&E.

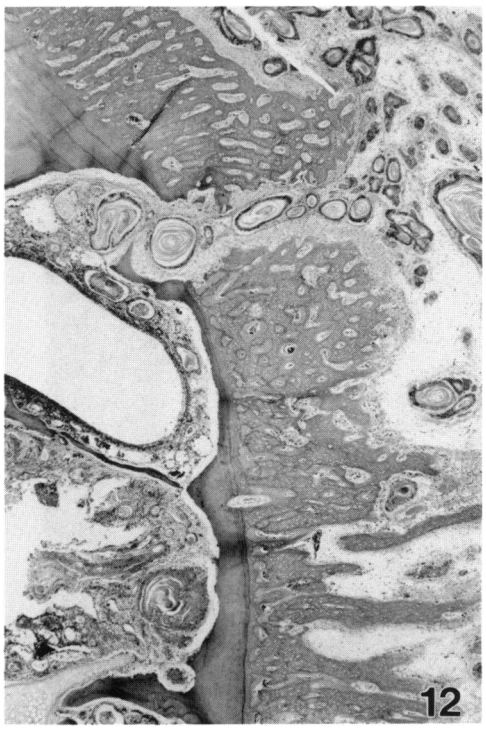

PLATE 12. Enlargement of Plate 10 showing the penetration of neoplastic cells through the frontal bone and keratin pearl formation. H&E.

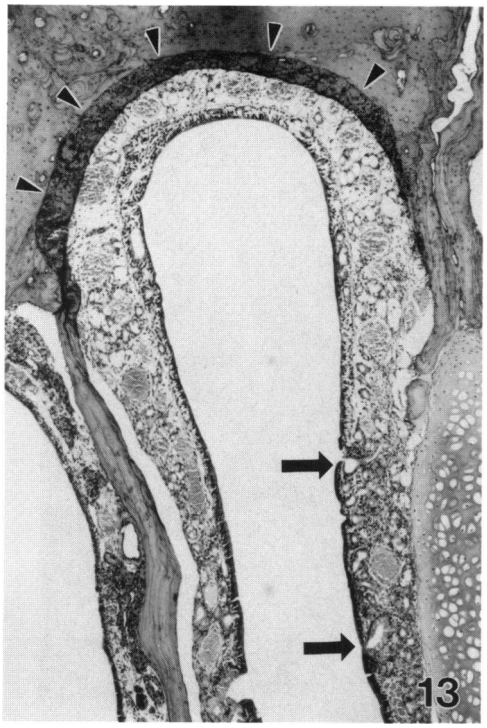

PLATE 13. Low magnification of a dorsal arch in Case 6. Invaginations of the hyperplastic mucosal epithelium are present along dorsal aspects of the nasal septum (large arrows). A common histologic artifact, overlapping of the frontal bone on the olfactory mucosa, is evident (small arrows). H&E.

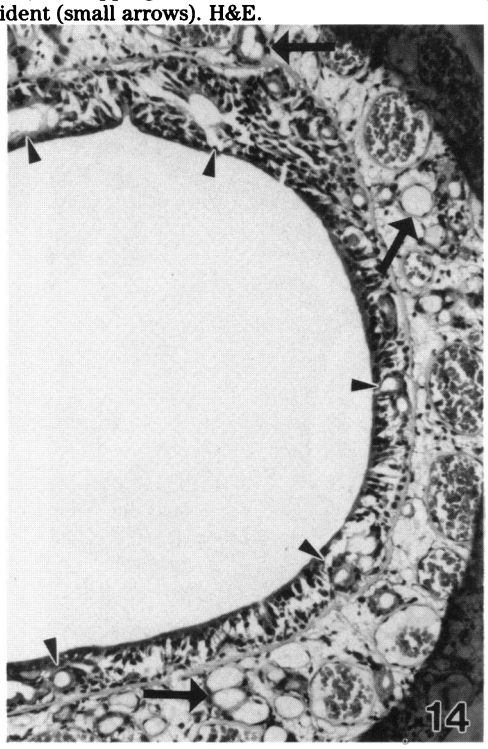

PLATE 14. Higher magnification of Figure 13 showing the loss of neuroepithelial cells, pseudogal and formation (small arrows), and dilated Bowman's glands (large arrows). H&E.

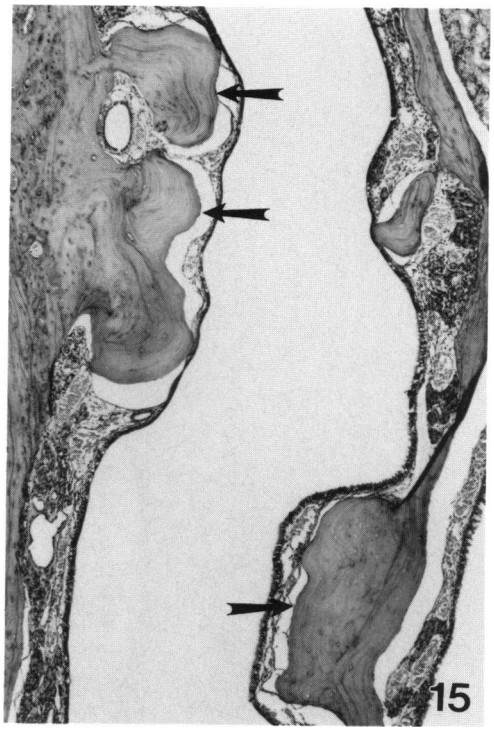

PLATE 15. High magnification of the lateral wall and nasoturbinate of Case 6 showing hyperostosis (large arrows). H&E.

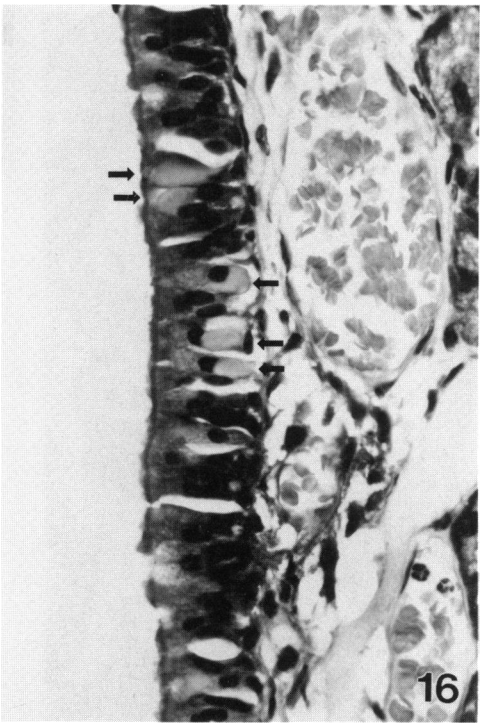

PLATE 16. Eosinophilic cytoplasmic inclusions (arrows) are present in the respiratory epithelium lining the nasal septum in Case 6. H&E.

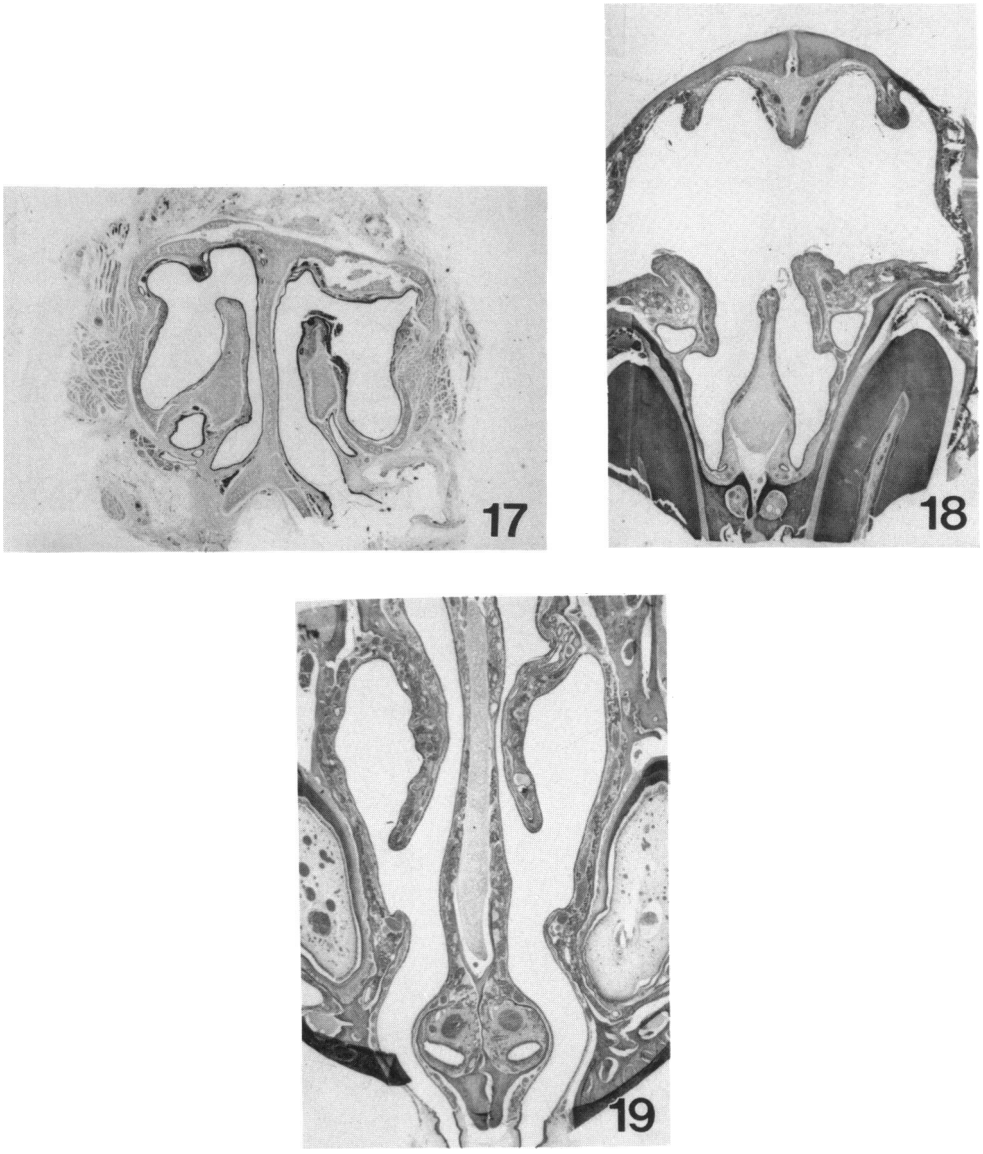

PLATE 17 through 19. Photomicrographs of three levels of the nose in Case 7. The middle level (Plate 18) is characterized by absence of an intact nasal septum and atrophy of naso- and maxilloturbinates. H&E stain was used. H&E.

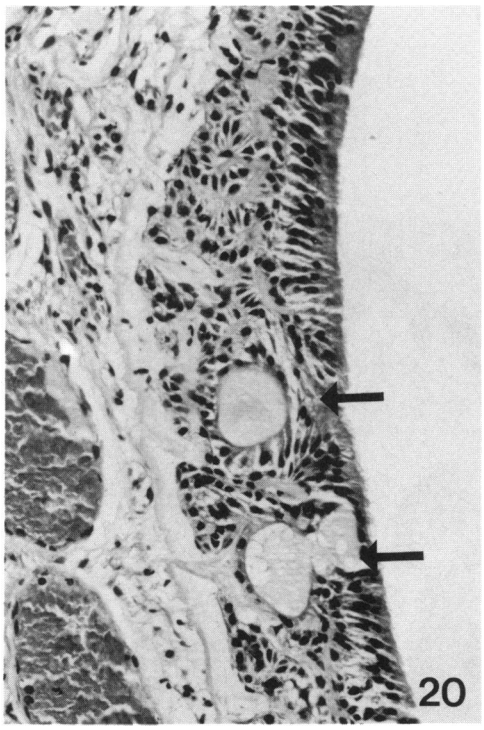

PLATE 20. High magnification of the dorsal arches from Plate 19. There is loss of neuroepithelium, cystic dilation of Bowman's glands (large arrows), and hyperplasia of Bowman's glands (small arrows). H&E.

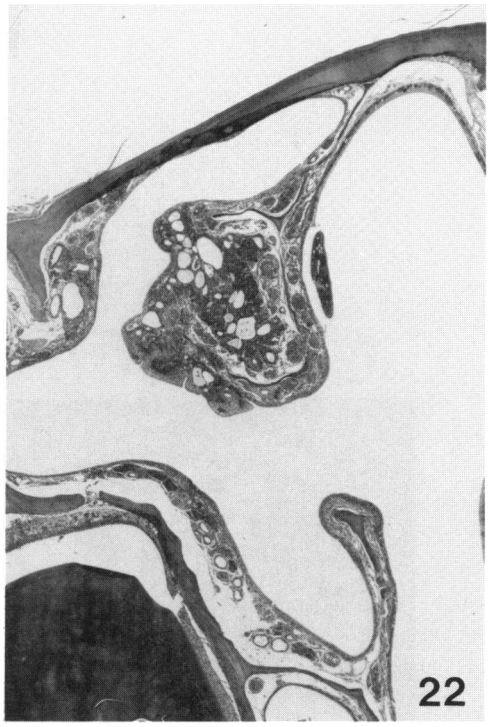

PLATE 22. Photomicrograph showing the larger of two polypoid adenomas in Case 8. H&E.

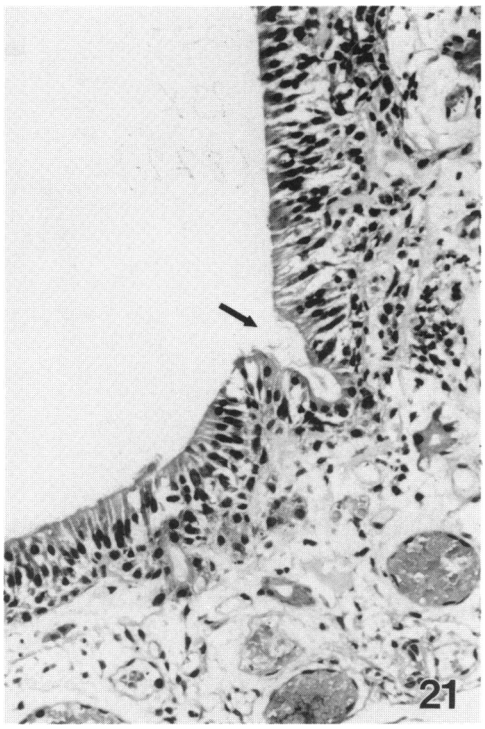

PLATE 21. High magnification of the dorsal arches from Plate 19 showing focal invagination of the olfactory epithelial mucosa (arrow). H&E.

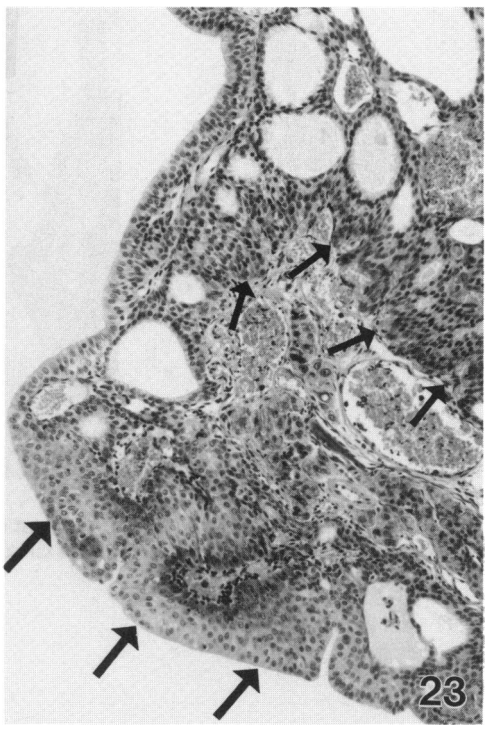

PLATE 23. Higher magnification of Plate 22 showing the proliferation of squamoid cells (large arrows) and smaller basal cells (small arrows). H&E.

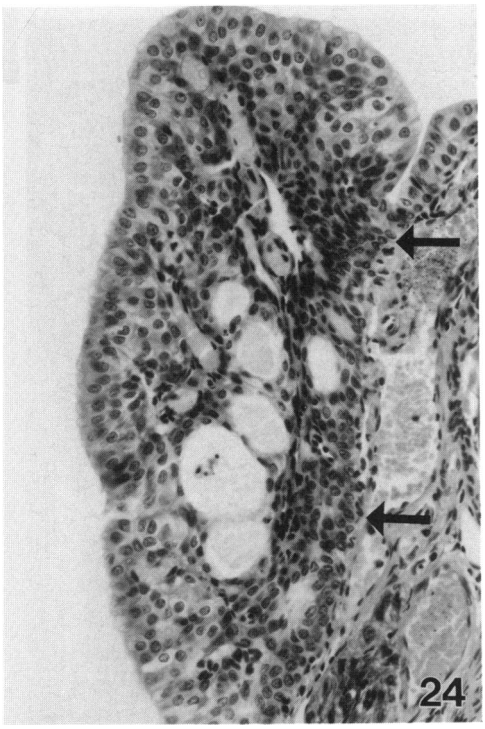

PLATE 24. High magnification of the smaller polypoid adenoma in Case 8 showing proliferation of squamoid cells and smaller basal cells (arrows). H&E.

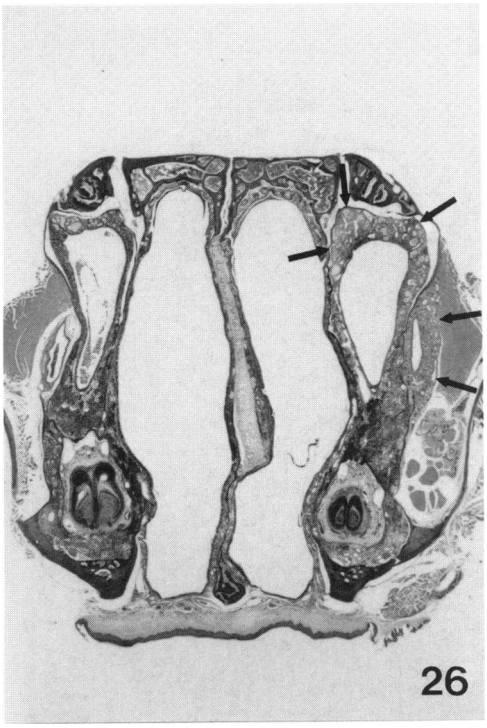

PLATE 26. Photomicrograph of Case 9 showing a thickening of the maxillary sinus and nasolacrimal duct mucosa (arrows). H&E.

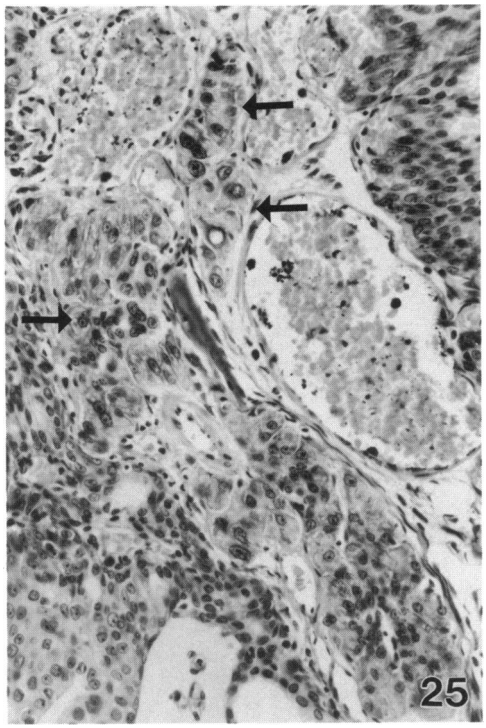

PLATE 25. High magnification of Plate 23 showing nuclear pleomorphism and hyperchromaticity of nuclei in reactive mucosal glands (arrows). H&E.

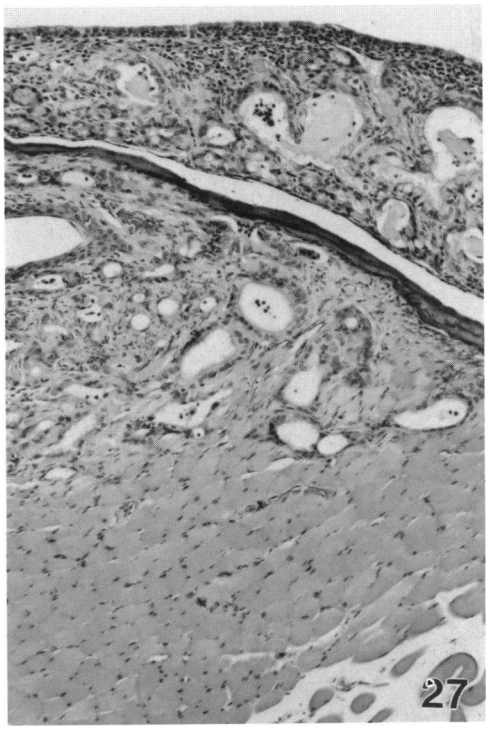

PLATE 27. High magnification of Plate 26 showing invasion of skeletal muscle by well-formed glands lined by ciliated epithelium. H&E.

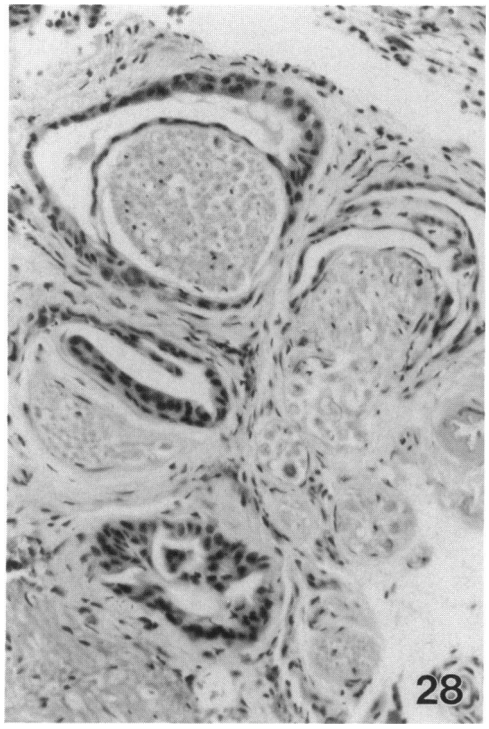

PLATE 28. High magnification of Plate 26 showing proliferating glands around nerve bundles. H&E.

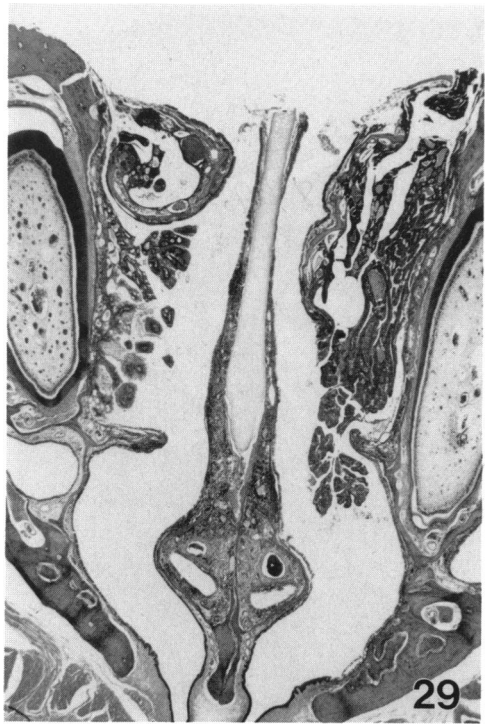

PLATE 29. Bilateral polypoid proliferations arising from the lateral walls of the anterior nasal cavity in Case 10. Overlying bone has been removed from the roof of the nasal cavity. H&E.

PLATE 30. Invasive proliferation of basophilic epitheliallike cells in the nasal septum of Case 10 with perineural invasion (arrows). H&E.

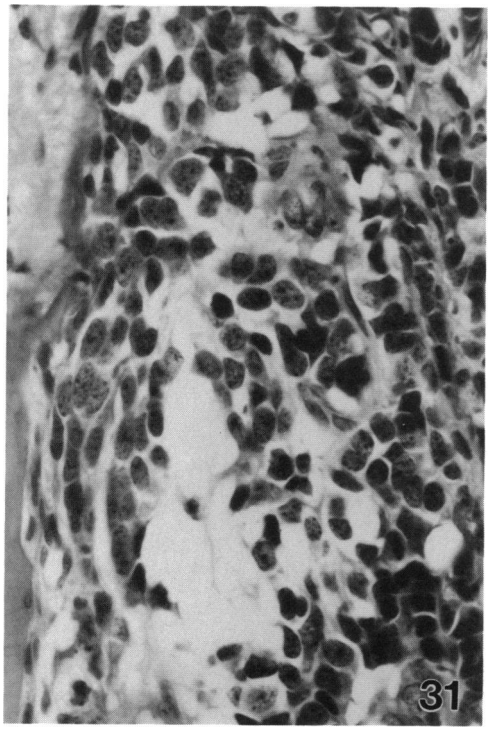

PLATE 31. Higher magnification of Plate 30 showing details of the proliferating basophilic epitheliallike cells in the nasal septum. H&E.

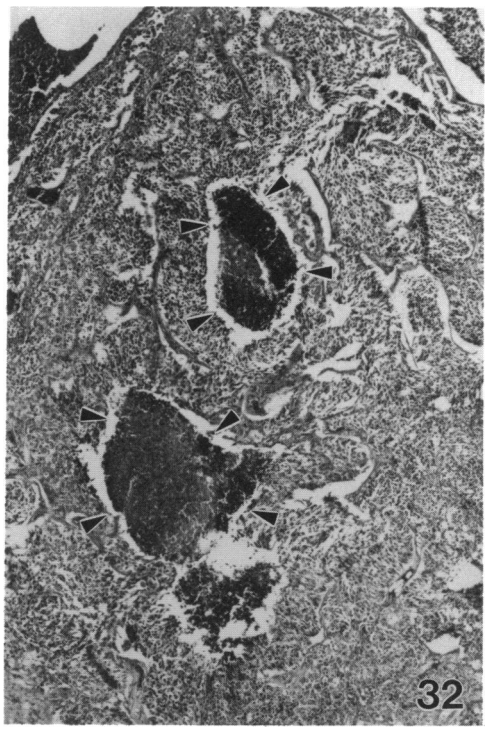

PLATE 32. Photomicrograph of a large mass with areas of necrosis (arrows) filling half of the nasal cavity in Case 11. H&E.

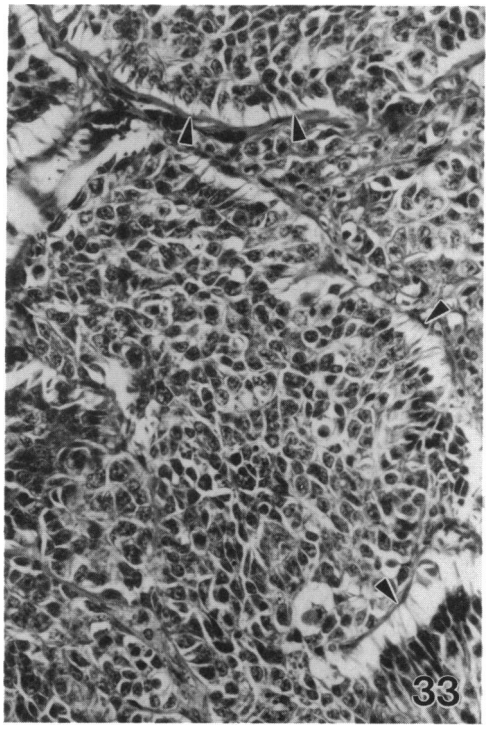

PLATE 33. Higher magnification of Plate 32 showing cells connected by cytoplasmic filaments to delicate connective tissue septae. H&E.

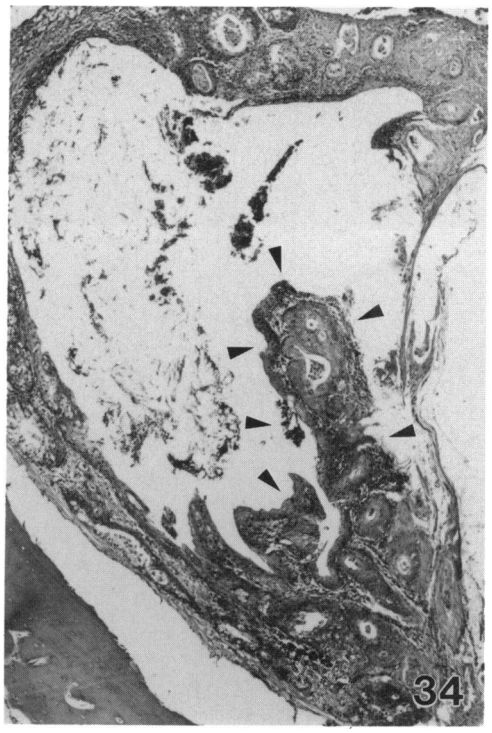

PLATE 34. Papillary proliferation (arrows) in the nasolacrimal duct of Case 11. H&E.

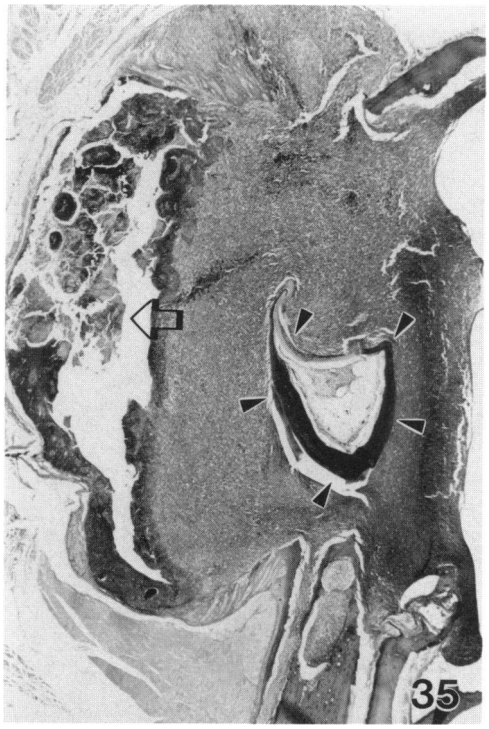

PLATE 35. Photomicrograph of a large proliferative mass occupying half the nasal cavity in Case 12. There is an accompanying proliferative response in the nasolacrimal duct (open arrow). The mass completely surrounds the incisor tooth (small arrows). H&E.

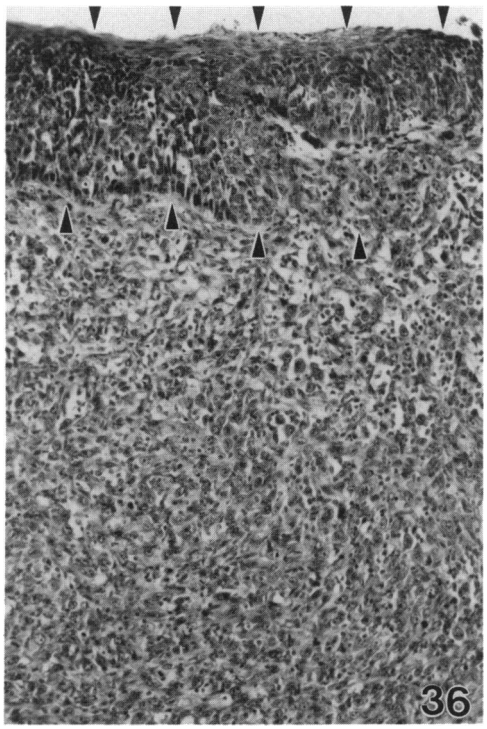

PLATE 36. High magnification of Plate 35 showing cytological features of the proliferating cells adjacent to the thickened epithelial mucosa (arrows) of the nasolacrimal duct. H&E.

PLATE 38. High magnification of Plate 37 showing thickening of an ethmoid turbinate by proliferating squamous cells. There is keratinization of the surface epithelium and intercellular bridges (desmosomes) are present in the more basal layers. H&E.

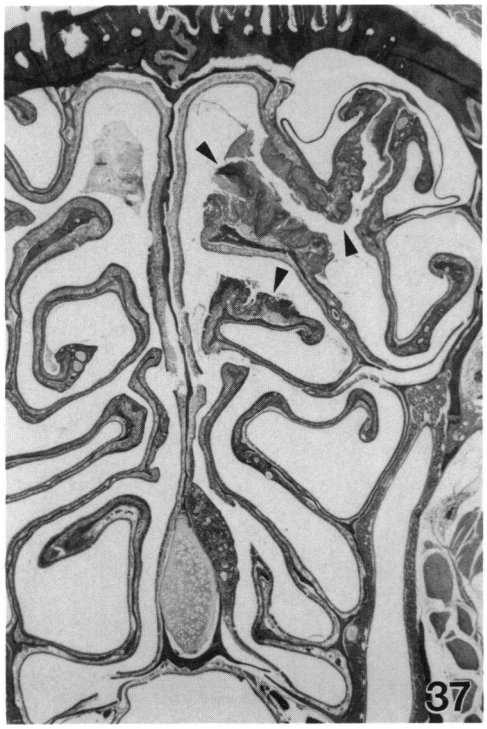

PLATE 37. Photomicrograph of the olfactory turbinates in Case 13. There is epithelial proliferation causing focal thickening of the ethmoid turbinates (arrows). H&E.

PLATE 39. High magnification of Plate 37 depicting an area of ethmoid turbinate thickening where the proliferating cells are forming glandlike structures. H&E.

PLATE 40. High magnification of Plate 37 showing an area of early proliferation of squamoid cells (arrows) that appear to be arising from the basal cell layer of the olfactory epithelium. H&E.

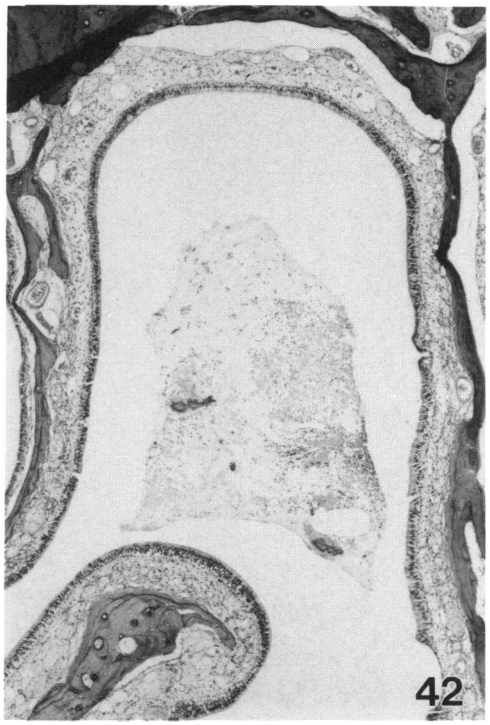

PLATE 42. Photomicrograph of the dorsal arch in the olfactory area of Case 13. H&E.

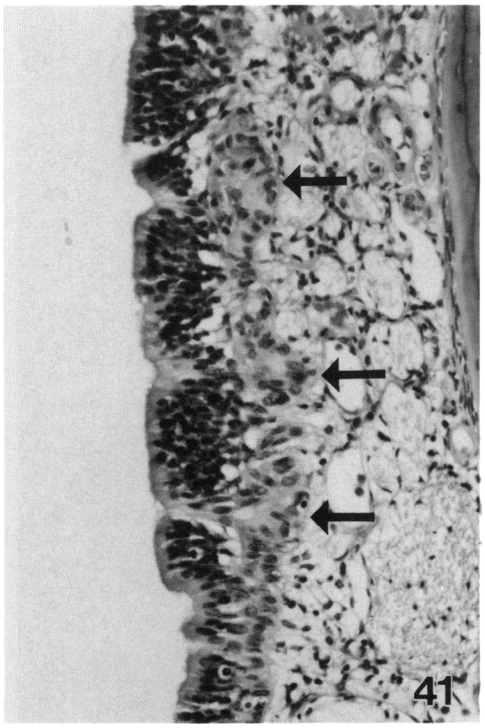

PLATE 41. High magnification of Plate 37 showing early proliferation of cells in what may represent residual Bowman's glands (arrows). H&E.

PLATE 43. High magnification of Plate 42 showing absence of Bowman's glands in the mucosa, degeneration of the olfactory epithelium, and respiratory metaplasia of the olfactory mucosa. H&E.

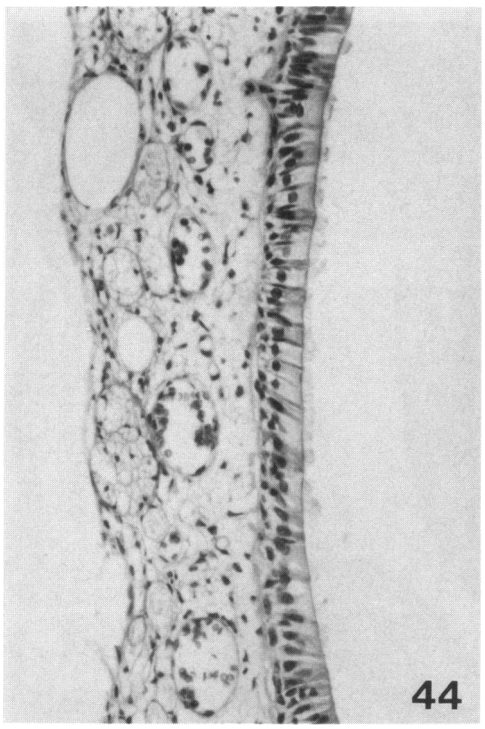

PLATE 44. High magnification of Plate 43 showing respiratory metaplasia of the olfactory mucosa. H&E.

PLATE 45. Photomicrograph of Case 14 showing infiltration of the mucosa overlying the dorsal meatus. Infiltrating cells are arranged in poorly defined nests. Remnants of olfactory epithelium are present (arrows). H&E.

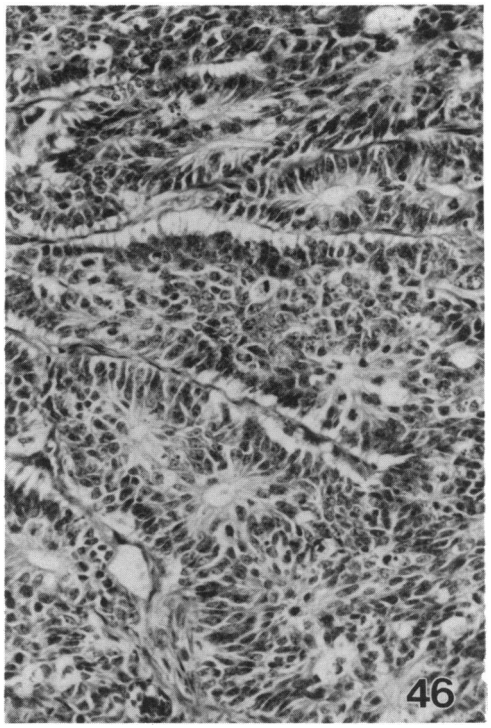

PLATE 46. Photomicrograph of Case 15 showing irregular packets of epithelial cells separated by thin connective tissue septae. The basal cells in these packets are attached to the connective tissue septae by delicate cytoplasmic filaments. H&E.

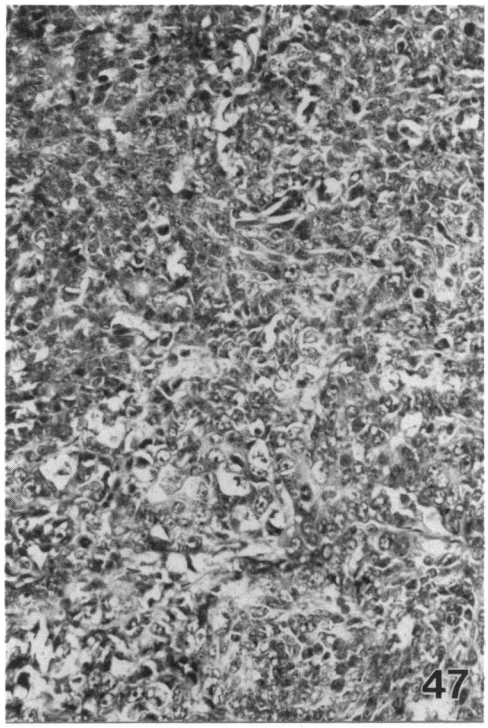

PLATE 47. High magnification photomicrograph of Case 15 from an area of epithelial proliferation where anaplastic epithelial cells are growing in sheets. H&E.

PLATE 48. Photomicrograph of thickened ethmoid turbinates in Case 16. H&E.

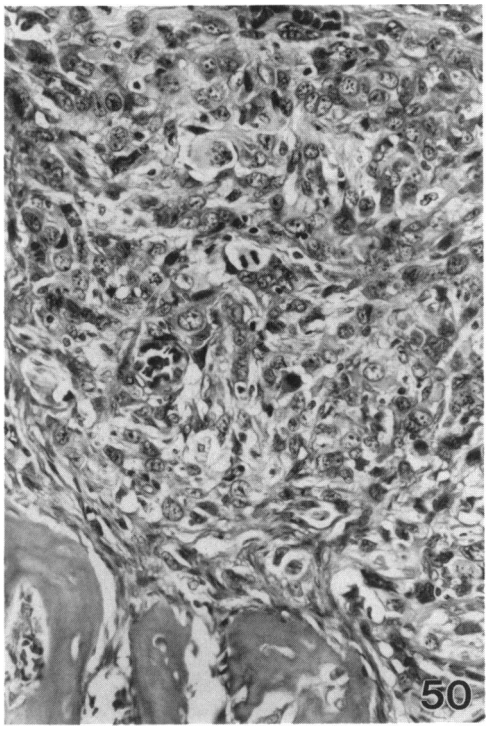

PLATE 50. Higher magnification of Plate 49 to show cytologic details of the anaplastic epithelial cells. H&E.

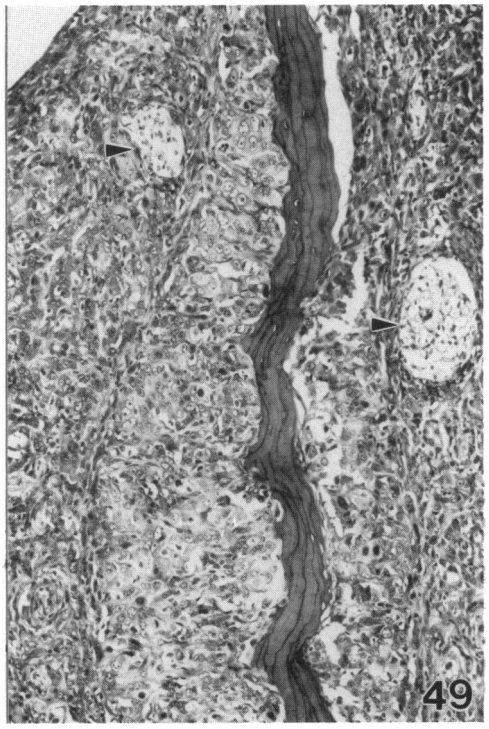

PLATE 49. High magnification of Plate 48 showing locally invasive anaplastic carcinoma cells. There is a relative sparing of the nerve bundles (arrows). H&E.

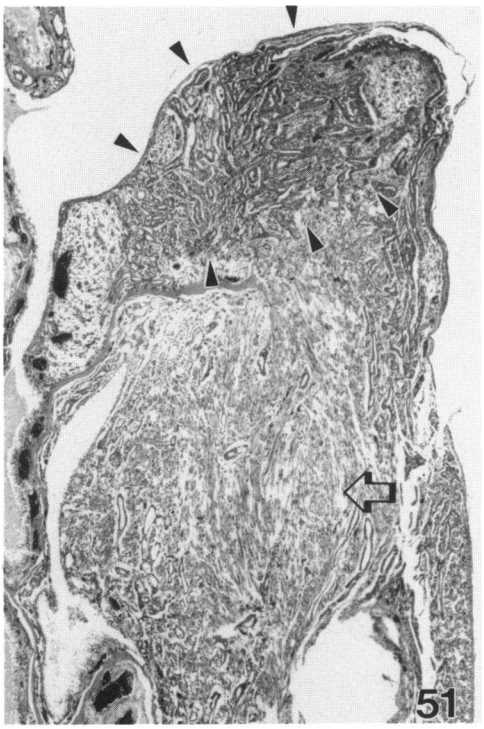

PLATE 51. Photomicrograph of the nasal mass in Case 17. Predominantely glandular patterns of growth are present in some portions of the neoplasm (small arrows), whereas mesenchymal cells are localized in other areas (open arrow). H&E.

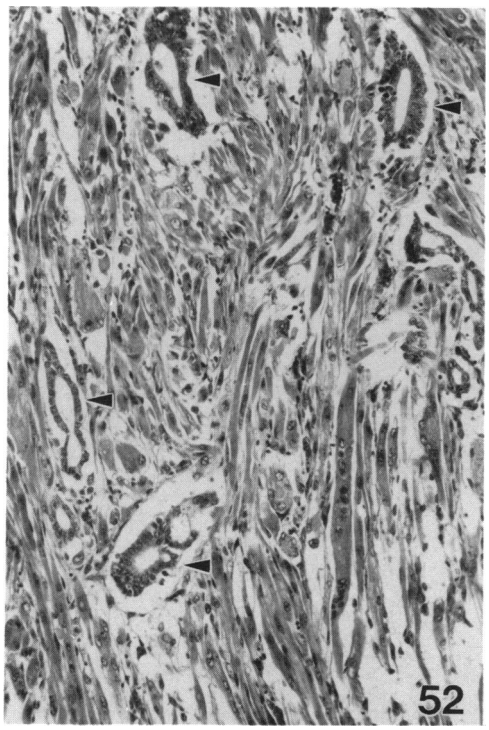

PLATE 52. High magnification of the central portion of Plate 51 showing proliferating glands (arrows) admixed with neoplastic skeletal muscle cells. H&E.

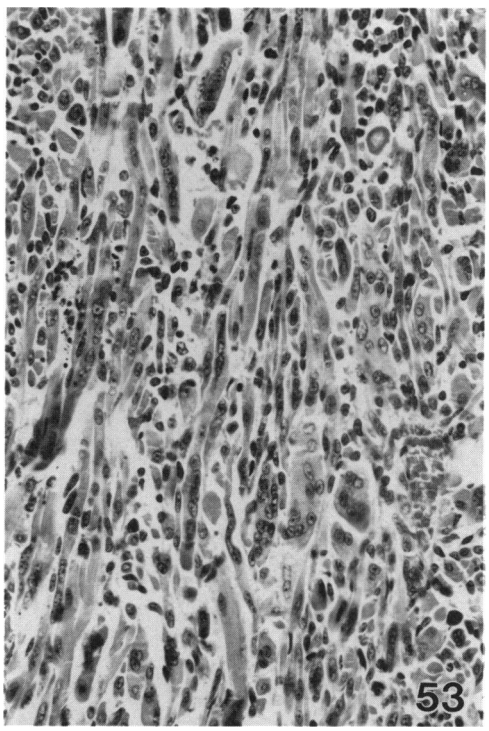

PLATE 53. Photomicrograph from Case 18 showing neoplastic skeletal muscle. H&E.